Interactions of Model Human Pulmonary Surfactants with a Mixed Phospholipid Bilayer Assembly: Raman Spectroscopic Studies

James S. Vincent,[‡] Susan D. Revak,[§] Charles D. Cochrane,[§] and Ira W. Levin*,[‖]

Chemistry Department, University of Maryland Baltimore County, 5401 Wilkens Avenue, Catonsville, Maryland 21228, Department of Immunology, Research Institute of Scripps Clinic, La Jolla, California 92037, and Laboratory of Chemical Physics, National Institute of Diabetes and Digestive and Kidney Diseases, National Institutes of Health, Bethesda, Maryland 20892

Received October 15, 1992; Revised Manuscript Received May 14, 1993

ABSTRACT: The temperature dependence and acyl chain packing properties of the binary lipid mixtures of dipalmitoylphosphatidylcholine-d_{62} (DPPC-d_{62})/dipalmitoylphosphatidylglycerol (DPPG) multilayers, reconstituted with two synthetic peptides for modeling the membrane behavior of the SP-B protein associated with human pulmonary surfactant, were investigated by vibrational Raman spectroscopy. The synthetic peptides consisted of 21 amino acid residues representing repeating charged units of either lysine or aspartic acid separated by hydrophobic domains consisting of four leucines (KL_4 or DL_4, respectively). These peptides were designed to mimic the alternating hydrophobic and hydrophilic sequences defining the low molecular weight SP-B protein. Raman spectroscopic parameters consisting of integrated band intensities, line widths, and relative peak height intensity ratios were used to probe the bilayer order/disorder characteristics of the liposomal perturbations reflected by the reconstituted membrane assemblies. Temperature profiles derived from the various Raman intensity parameters for the 3100–2800-cm^{-1} carbon–hydrogen (C–H) and the 2000–2300-cm^{-1} carbon–deuterium (C–D) stretching mode regions, spectral intervals representative of acyl chain vibrations, reflected lipid reorganizations specific to peptide interactions with either the DPPC-d_{62} or DPPG component of the liposome. For the multilamellar surfactant systems composed of either KL_4 or DL_4 reconstituted with the binary DPPG/DPPC-d_{62} lipid mixture, the breadth of the gel to liquid crystalline phase transition temperatures T_M, defined by acyl chain C–H and C–D stretching mode order/disorder parameters, increased from about 1 °C in the peptide-free systems to over 10 °C. This breadth in T_M indicates an increased lipid disorder and a distinct noncooperative chain melting process for the model liposomes. In comparing the interactions of the synthetic peptides with DPPG/DPPC mixtures and with DPPC liposomes alone, the negatively charged DL_4 peptide perturbs the DPPG component of the lipid mixture more strongly than the DPPC-d_{62} component; moreover, the DL_4 peptide disrupts the structure of the DPPG lipid domains in the binary mixture to a greater extent than the KL_4 peptide. The microdomain heterogeneity of the binary lipid mixture arising from lipid–peptide interactions is discussed in terms of the Raman spectral properties of the multilayers. The Raman data in conjunction with previous bubble surfactometer and animal studies (Cochrane & Revak, 1991) suggest that lipid domain structures are present in functional surfactants and that the dynamic bilayer microheterogeneity induced by the surfactant peptide or protein is essential for pulmonary mechanics.

The major constituents of pulmonary surfactant are a mixture of phospholipids and specific low molecular weight proteins. Protein interaction with the lipid mixture serves to decrease the surface tension of the surfactant lining the alveoli, preventing both the collapse of the lung and edema during the expiration of air (Clements, 1977). Produced by type II pneumocyte cells, the surfactant is stored until required in tubular myelin structures in the alveolar lining just below the air–hypophase boundary (Scarpelli, 1988). Major constituents of the surfactant include dipalmitoylphosphatidylcholine (DPPC)[1] and various phosphatidylglycerols (PG), with the associated proteins, SP-A, SP-B, SP-C (Harwood & Richards, 1985), and a newly discovered collagenous glycoprotein, SP-D (Persson et al., 1990). Recent studies have focused on phospholipid mixtures with either SP-B residues or synthetic peptide paradigms as substitutes for natural surfactant in the treatment of respiratory distress syndrome in laboratory animals (Revak et al., 1988, 1991; Cochrane & Revak, 1991). However, for discerning the specific molecular interactions necessary to induce adequate surface tension behavior in the development of surfactant replacement therapies, the design of relatively short synthetic peptide sequences proves to be more tractable. The most efficacious synthetic peptides for demonstrating surface tension-lowering properties on binary lipid mixtures are those which model the punctuated hydrophobic and hydrophilic sequences present in the native SP-B protein (Cochrane & Revak, 1991). For example, the addition of peptides, containing either arginine or lysine as the charged residues and stretches of leucines for the hydrophobic units, to DPPC/PG phospholipid mixtures greatly reduces the surface tension properties of the lipid assembly in bubble surfactometer studies (Vincent et al., 1991; Cochrane & Revak, 1991). Additionally, fetal rabbit lungs exhibit a nearly

* Correspondence should be addressed to this author.
‡ University of Maryland Baltimore County.
§ Research Institute of Scripps Clinic.
‖ NIDDK, NIH.

[1] Abbreviations: DPPC, dipalmitoylphosphatidylcholine; DMPC, dimyristoylphosphatidylcholine; DPPC-d_{62}, dipalmitoylphosphatidylcholine with perdeuterated acyl chains; DPPG, dipalmitoylphosphatidylglycerol; DL_4, DLLLDLLLDLLLDLLLD; D, aspartic acid; L, leucine; KL_4, KLLLKLLLKLLLKLLLK; K, lysine; PLL, poly(L-lysine); SP, surfactant protein.

0006-2960/93/0432-8228$04.00/0

3-fold increase in compliance (volume air flow per pressure per unit body weight) in the presence of the synthetic surfactant material (Cochrane & Revak, 1991). A recent spectroscopic investigation of a 3:1 mixture of DPPC and egg PG, to which was added either a portion of SP-B protein or peptide sequences composed of arginine and leucine domains, showed a slight increase in the gel to liquid crystalline phase transition temperature, T_M, of the lipid multilayer system and a decreased cooperativity of the phase transition in comparison with the peptide-free lipid mixture (Vincent et al., 1991). An interpretation of that study suggested that electrostatic headgroup interactions between the charged regions of the synthetic peptides and the PG component of the binary lipid mixture induced partial segregation of the bilayer into both PG- and DPPC-rich domains. In the present study, we elucidate further the mechanisms of lipid bilayer domain formation within the multilamellar assemblies in the presence of synthetic peptides. Surfactant material is comprised specifically of 21 amino acid residues whose sequences alternate between charged domains of either lysine (K) or aspartic acid (D) and hydrophobic regions of leucines (L), while the binary lipid mixture consists of a 1:1 mole ratio system of dipalmitoylphosphatidylglycerol (DPPG) and DPPC-d_{62} in which the DPPC acyl chains are completely deuterated. If the hydrocarbon chain regions of each lipid class are separately labeled, perturbations by the peptides to the bilayer interior can be assessed in detail. This strategy allows determinations concerning bilayer heterogeneity and putative lateral lipid segregation.

Vibrational Raman spectroscopy is particularly well suited for studying binary lipid systems as aqueous dispersions in which one component possesses perdeuterated acyl chains (Mendelsohn et al., 1978, 1980; Bryant et al., 1982). With the acyl chain methylene carbon–deuterium (C–D) vibrational modes occurring in spectral regions displaced from the acyl chain C–H vibrations, both lipid species can be monitored independently. This noninvasive Raman spectroscopic approach is an advantage for studying the thermotropic behavior of lipid membrane systems. The temperature dependence of several spectral peak height intensity ratios and integrated intensity parameters derived from the lipid acyl chain methylene and methyl C–H and C–D stretching modes reflect the inter- and intrachain order characteristic of the reconstituted multilayer assemblies (Levin, 1984, 1985). For example, the spectral carbon–hydrogen (C–H) peak height intensity ratio, I_{2850}/I_{2880}, where the 2850- and 2880-cm^{-1} modes refer to the acyl chain methylene CH_2 symmetric and asymmetric stretching vibrations, respectively, reflects the lateral chain–chain interactions defining the bilayer dynamics. Order/disorder measures also arising from chain–chain interactions, but with contributions from intrachain *trans*/*gauche* isomerizations, are determined from the I_{2935}/I_{2880} intensity parameter. The 2935-cm^{-1} feature represents a complex spectral interval that contains vibrational components from Fermi resonance interactions involving the chain methylene moieties and, separately, the C–H symmetric stretching modes of the chain methyl termini of the lipids comprising the liposomes (Hill & Levin, 1979). Other measures of lateral interchain interaction for the deuterated species are determined from line width parameters of the 2103-cm^{-1} perdeuterated acyl chain symmetric methylene C–D stretching modes; namely, $\Delta\nu_{7/8}$, the line width at $^7/_8$ of the peak intensity (Devlin & Levin, 1990). The halfwidth parameter ($\Delta\nu_{1/2}$) for the 2103-cm^{-1} band reflects predominantly intrachain *trans*/*gauche* isomerization disorder and increases proportionally to the number of *gauche* conformers induced along the lipid hydrocarbon moiety (Bryant et al., 1982; Mendelsohn & Koch, 1980).

MATERIALS AND METHODS

Synthetic L-α-dipalmitoylphosphatidylcholine-d_{62} (DPPC-d_{62}) and dipalmitoylphosphatidylglycerol (DPPG) were obtained from Avanti Polar Lipids and used without further purification. Multilayer dispersions of the 1:1 mole ratio mixture of DPPC-d_{62} and DPPG were prepared according to previous studies (Revak et al., 1988, 1991) by first dissolving the lipids in a mixture of chloroform and methanol and evaporating the solvent first under a nitrogen flow and finally under high vacuum. Water is added to disperse the lipid and the mixture is incubated, accompanied by gentle mixing, for an hour at 43 °C in the liquid-crystalline phase. A saline buffer solution, (0.15 M Tris, acetic acid, NaCl, pH 7.20) is added to restore isotonicity, and the resulting dispersion is subjected to three freeze–thaw cycles through the phase transition. After the samples were sealed in glass capillary tubes, the multilayers were compacted in a hematocrit centrifuge. In cases where the lipid samples were gelatinous and did not compact easily, the dispersions were centrifuged in a Beckmann Ultracentrifuge for 20 min at 80000*g*. Samples were stored in a refrigerator at 2–5 °C for at least 24 h before recording the spectra.

The specific peptide sequences, KL_4 (KLLLLKLLLL-KLLLLKLLLK) and DL_4 (DLLLLDLLLLDLLLLD-LLLLD), where K, D, and L are the standard symbols for lysine, aspartic acid, and leucine, respectively, were synthesized following the methods of Merrifield (1963) as described previously (Revak et al., 1991). Peptide/lipid multilayers (4.8% weight peptide) were reconstituted by adding 1 mg of peptide to 20 mg of lipid mixture of DPPC-d_{62} and DPPG in the chloroform/methanol solvent mixture. (The approximate mole ratio of lipid to peptide for the two systems is greater than 60:1). After the solvent was evaporated under a stream of nitrogen at 40 °C, all final traces of the solvent mixture were removed under vacuum. Subsequent treatment for preparing the peptide/lipid dispersions followed the same procedures described above. Since the lipid/peptide mole ratio of the reconstituted systems are of the order of 60:1, examination of the Raman spectra of the multilayers indicated that no protein subtractions were required for determining unoccluded lipid spectra in the C–H stretching mode interval.

Laser excitation at 514.5 nm, obtained from a Coherent Innova 100 Argon unit, ranged from 150 to 300 mW at the sample for the Raman spectrophotometric experiments. No evidence of local heating effects in the samples was observed at these laser power levels. The scattered light was collected with a Spex Ramalog double spectrometer at a spectral resolution of $\sim$5 cm^{-1} and was detected with a thermoelectrically cooled RCA C31034 photomultiplier tube. Raman spectra were observed as a function of temperature at 1.0 °C intervals from approximately 25 to 55 °C. The specific temperature range varied between experiments. A thermostated bath circulated heat exchanged fluid through a thermoelectrically controlled sample holder, which also housed the thermocouple used for monitoring the bath temperature. A separate solid-state temperature-sensitive device controlled the power supplied to the thermoelectric temperature regulator. The Raman scattering, temperature bath control, spectral scan rate, and span were recorded and controlled, respectively, with a PC-based laboratory computer system. Spectral files were transferred to a SUN workstation over the local network for both data storage and spectral manipulation. The data

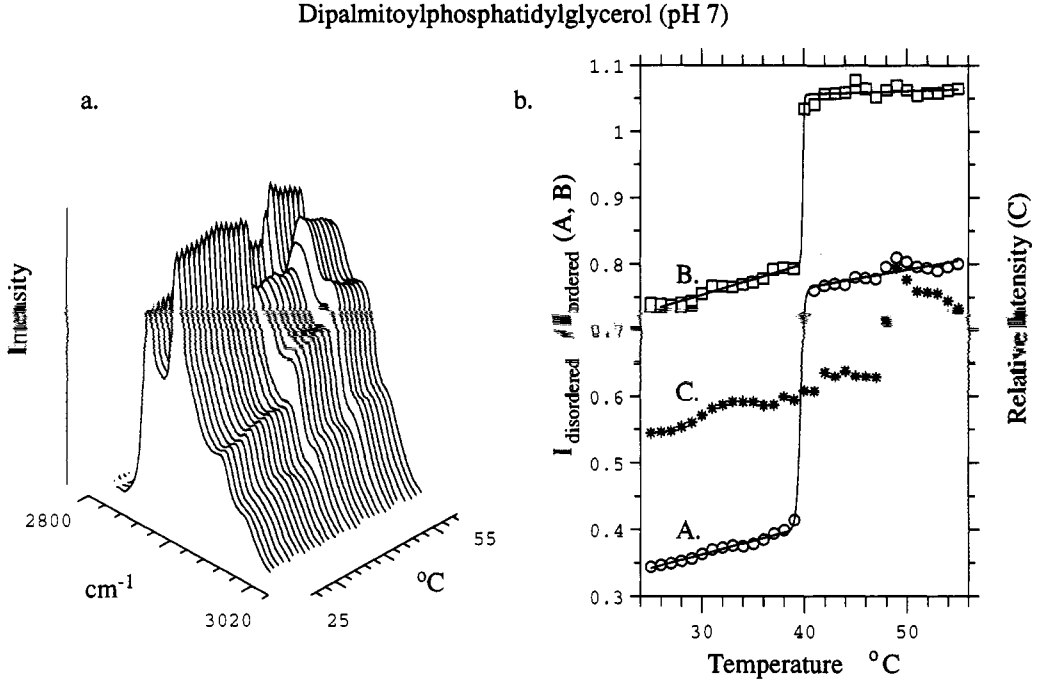

FIGURE 1: Raman spectra of DPPG in the C–H stretching mode region (2800–3000 cm^{-1}) as a function of temperature. (a) Topological plot of pure DPPG at pH 7.2 in isotonic NaCl solution. (b) Peak height intensity ratios: (A) I_{2935}/I_{2880}; (B) I_{2850}/I_{2880}. (C) Relative integrated intensity over the C–H stretching mode region. The lines were calculated using a two-state model for lipid transitions (Kirchhoff & Levin, 1987) to fit the experimental points in A and B.

given in the figures and Table I are representative of at least two sample preparations in the case of the peptide mixtures and from many samples of the pure DPPC and DPPG multilamellar vesicles.

RESULTS AND DISCUSSION

Pure DPPG and DPPC-d_{62} Bilayers. For the purposes of comparing the order/disorder properties of the surfactant/lipid multilamellar assembles, we first present the Raman spectral results of the individual lipid components, the lipid mixture, and then the surfactant/lipid mixtures. Raman scattering profiles of the pure DPPG liposomes at pH 7 are shown as a function of temperature in Figure 1a. The in-plane axes represent the wavenumber and temperature values, while the intensity of the Raman scattering is graphed on the out-of-plane axis. The C–H stretching mode parameters represented by the I_{2935}/I_{2880} intensity ratio, which contains contributions from *gauche/trans* isomerizations superimposed upon lateral chain–chain interactions, the I_{2850}/I_{2880} intensity ratio, reflecting interchain interactions and acyl chain packing arrangements, and the relative integrated intensities over the C–H stretching mode region are illustrated in Figure 1, panels bA, bB, and bC, respectively. The integrated intensity parameter is a function of the number of molecular scatterers in the exciting laser beam and of the polarizability changes of the molecules induced by the various vibrational displacement coordinates. (We find it more useful to monitor relative changes in the total integrated intensity of the Raman emission over the entire 2800–3100-cm^{-1} or 2000–2300-cm^{-1} interval rather than to attempt spectral deconvolutions and individual band integrations over this complex manifold of vibrational transitions.)

The determination of T_M and the gel to liquid crystalline phase transition widths, ΔT, by analysis of the Raman spectral temperature behavior assumes that the spectral parameter (intensity ratio I_{2935}/I_{2880}, or I_{2850}/I_{2880} in this case) depends upon the distribution between the two states of the observed molecules and is given by

$$\frac{I_1}{I_2} = \frac{A + a(T - T_M)}{(1 + e^{+t})} + \frac{B + b(T - T_M)}{(1 + e^{-t})}$$

in which $t = (T - T_M)/D$ and A, B, a, b, D, and T_M are fit by a least-squares criterion to the data (Kirchhoff & Levin, 1987). The width of the transition ΔT is given by $4D$ and the phase transition temperature is represented by T_M. D is related to the enthalpy of the transition per mole of lipid, ΔH, and the domain size of the melting cluster, n, by

$$D = (RT_M^2)/(\Delta Hn)$$

With the existing quality of data and density of points, the estimated errors in T_M are less than 0.3 °C. The reported error for each parameter is the square root of the variance, a value close to the standard deviation for this number of data points. Table I summarizes the gel to liquid crystalline phase transition parameters T_M and ΔT for DPPG and DPPC-d_{62}; the gel and liquid crystalline peak height ratios listed in Table I pertain to those values at 15 °C below and above T_M, respectively.

Literature values for T_M for pure DPPG liposomes, determined calorimetrically, range between 39.5 and 41.5 °C (Findlay & Barton, 1978; Van Dijek et al., 1978; Jacobson & Papahadjopoulos, 1975; Van Dijck, 1979). Carrier and Pézolet (1984) obtain a value of 40 °C from Raman spectroscopic techniques, which is in good agreement with our value of 39.6 ± 0.2 °C. (Our data exhibit a small pretransition at 31 °C in comparison to Carrier and Pézolet's (1984) value of ~33 °C). The slight depression for T_m observed in the present study, in comparison to Carrier and Pézolet's (1984) Raman data, may indicate interactions with the buffered saline solution which we add to restore physiological conditions, since our experiments precluded any local laser heating effects. The integrated intensity curve (Figure 1bC) shows minimal change at the gel to liquid crystalline phase transition. However, there is a large change in the

Table I: Raman Spectral Parameters for Multilamellar Vesicles Composed of the Peptides KL_4 or DL_4 in 1:1 Mixtures of Dipalmitoylphosphatidylglycerol and Dipalmitoylphosphatidylcholine-d_{62}, the Phospholipid Mixture without the Peptides and the Separate Phospholipids at pH 7

	peak height intensity ratios, DPPG, DPPC								line width (cm^{-1}), DPPC-d_{62}							
	I_{2935}/I_{2880}				I_{2850}/I_{2880}				$\Delta\nu_{1/2}$				$\Delta\nu_{7/8}$			
	phase[a]				phase[a]				phase[a]				phase[a]			
sample	gel	LC	T_M (°C)[b]	ΔT (°C)[b]	gel	LC	T_M (°C)	ΔT (°C)	gel	LC	T_M (°C)	ΔT (°C)	gel	LC	T_M (°C)	ΔT (°C)
DPPG	0.35	0.80	39.6 ± 0.2	0.8 ± 0.2	0.73	1.06	39.9 ± 0.2	0.7 ± 0.2								
DPPC-d_{62}[c]									30	42	35.2 ± 0.2	<1.0	11	15.4	35.3 ± 0.2	1.8 ± 0.6
1:1 DPPG+DPPC-d_{62}	0.40	0.80	37.1 ± 0.2	2.2 ± 0.4	0.87	1.15	37.0 ± 0.3	2.4 ± 0.7	29	43	36.8 ± 0.3	2.5 ± 0.8	10	14	37.2 ± 0.4	4.6 ± 1.1
mixture[d]+KL_4	0.55	0.92	38–40[e]	18	0.92	1.07	37–39	13	29	42	37–39	12	11	14	37–40	10
mixture[d]+DL_4	0.60	1.0	38–40	18	0.84	0.97	38–40	14	29	43	38–40	16	11	14	38–42	14
DPPC-d_0	0.46	0.83	41.3 ± 0.2	0.9 ± 0.1	0.78	0.95	41.4 ± 0.2	1.1 ± 0.1								
DPPC+DL_4	0.53	0.86	41.3 ± 0.2	3.2 ± 0.4	0.80	1.0	41.5 ± 0.2	2.2 ± 0.6								
DPPC+KL_4	0.47	0.88	39.4 ± 0.2	6.4 ± 0.7	0.77	1.04	39.9 U 0.3	5.6 ± 0.8								
DPPG+DL_4	0.62	0.98	40.1 ± 0.4	7.1 ± 1.2	0.68	0.84	39.1 ± 1.2	2.6 ± 1.8								
DPPG+KL_4	0.37	0.82	37.1 ± 0.3	2.8 ± 0.8	0.75	1.0	37.8 ± 0.2	2.2 ± 0.7								

[a] The listed intensity ratios and line widths are those 15 °C below the T_M and 15 °C above. Uncertainties are 0.02 for the peak ratios and 0.5 cm^{-1} for the line widths. The temperature ranges for T_M and ΔT are estimated (not fit) for the lipid mixture with DL_4 and KL_4. [b] The main phase transition temperatures T_M and widths of the phase transition ΔT with listed uncertainties were determined by fitting a theoretical sigmoidal curve derived from a two-state model for lipid phase transitions (Kirchhoff & Levin, 1987) to the peak height ratio data of the C–H stretching mode region and to the line width data of the C–D 2103-cm^{-1} feature for $\Delta\nu_{1/2}$ and $\Delta\nu_{7/8}$. Listed uncertainties are the square root of the parameter variances. [c] Data from Devlin and Levin (1990). [d] The lipid mixture in these cases is the 1:1 mole ratio mixture of DPPG and DPPC-d_{62}.

scattering intensity around 49 °C which is also replicated to a much smaller extent in the I_{2935}/I_{2880} peak intensity ratio plot (Figure 1bA). Normal phase transitions result in a lattice expansion due to an increased number of *gauche* conformers in the acyl chains, and this lattice expansion generally leads to a decrease in the Raman scattering intensity. In the DPPG system the scattering intensity remains constant throughout the phase transition and increases at a higher temperature. Lipid bilayer matrix contractions due to the partial dehydration of the headgroup may occur, providing a possible mechanism for this increase in scattering intensity. Hydrogen, ionic, and coordinate bond reorganizations within the glycerol headgroup may also increase the packing density of the multilayers while leaving the acyl chain disorder unchanged. Negatively charged lipids such as DPPG have phase transition parameters which are particularly sensitive to pH (Eibl & Wooley, 1979), compensating cation (Vincent & Levin, 1991), and ionic strength (Cevc et al., 1980).

Temperature profiles for pure DPPC-d_{62} multilayers have been investigated by us previously and have been discussed elsewhere (Devlin & Levin, 1990). Although DPPC-d_{62} packs isomorphously with DPPC-d_0 within the lipid aggregate, the T_M of DPPC-d_{62} is slightly lower than its -d_0 counterpart as a consequence of the difference in the zero point vibrational energy levels of the isotopic species. The data in Table I for DPPC-d_{62} are taken from Devlin and Levin (1990) and have been confirmed by spectra at specific temperatures. The breadth of the main phase transition (ΔT) for the pure multilamellar assembly is quite narrow (less than 1 °C, in general) for both lipid species, which is indicative of a large degree of cooperativity among neighboring molecules during the chain melting transition.

1:1 Mole Ratio DPPC-d_{62}/DPPG Binary Phospholipid Mixture. Although the 3100–2800-cm^{-1} C–H and the 2000–2300-cm^{-1} C–D stretching mode regions comprise a complex collection of vibrational modes, changes in the spectral intensities of these vibrations and the line widths as a function of bilayer perturbation and temperature reflect both inter- and intramolecular changes within the hydrophobic region of the membrane (Hill & Levin, 1979; Levin, 1984). Figure 2a presents a topological plot of the C–H stretching mode region for the DPPG portion of the lipid multilayers derived from the 1:1 DPPG/DPPC-d_{62} phospholipid mixture. As shown in this figure and the curve in Figure 2bC, the integrated intensity corresponding to this spectral interval increases gradually with temperature from 22 °C and reaches a maximum at approximately 37 °C, the same value as the T_M, as deduced from the sigmoidal plots of the peak heights intensity ratios shown in Figure 2, panels bA and bB. The integrated intensity curve decreases in intensity until a reasonably constant value is achieved at temperatures above 42 °C. The decrease in the integrated intensity parameter (Figure 2bC) correlates with decreasing bilayer order and lattice expansion and spans the gel to liquid crystalline phase transition, displayed by the temperature profiles in Figure 2, panels bA and bB. This integrated intensity response differs from that of the pure DPPG multilayer system shown in Figure 1bC. The peak intensity ratios of the 2935- and 2880-cm^{-1} features, I_{2935}/I_{2880}, displayed in Figure 2bA, increase toward greater multilamellar disorder with rising temperature. This spectral parameter reflects primarily interchain bilayer disorder with superimposed contributions from intrachain *trans/gauche* isomerization. The peak height intensity ratio parameter, I_{2850}/I_{2880}, reflecting pure lateral chain–chain interactions, also increases with temperature, as shown in Figure 2bB, in the same manner as the I_{2935}/I_{2880} parameter and yields essentially the same T_M. The spectral data for the 1:1 phospholipid mixture and for pure DPPC multilayers are summarized in Table I.

As determined by the values of the I_{2935}/I_{2880} and I_{2850}/I_{2880} peak height intensity ratios listed in Table I, DPPG in the lipid mixture exhibits both greater acyl chain intramolecular and lateral, intermolecular disorder in the gel phase than the pure saturated chain DPPG multilayers, although the intrachain order for DPPG is greater than that of pure DPPC-d_0 multilayers. The peak height ratios reflecting intrachain disorder are similar for the liquid-crystalline phases of the DPPG/DPPC-d_{62} mixture and the pure DPPG multilayer; the lateral disorder is definitely greater, however, for DPPG in the mixture in comparison to the pure multilayer liquid-crystalline disorder of DPPG. The Raman scattering of the C–D stretching mode spectral region for the DPPC-d_{62} species of the lipid mixture is displayed in Figure 2c and the derived line width parameters and integrated scattering intensity appear in Figure 2d. The T_M of 37.0 ± 0.3 °C for the lipid mixture, determined by I_{2850}/I_{2880} for DPPG, is

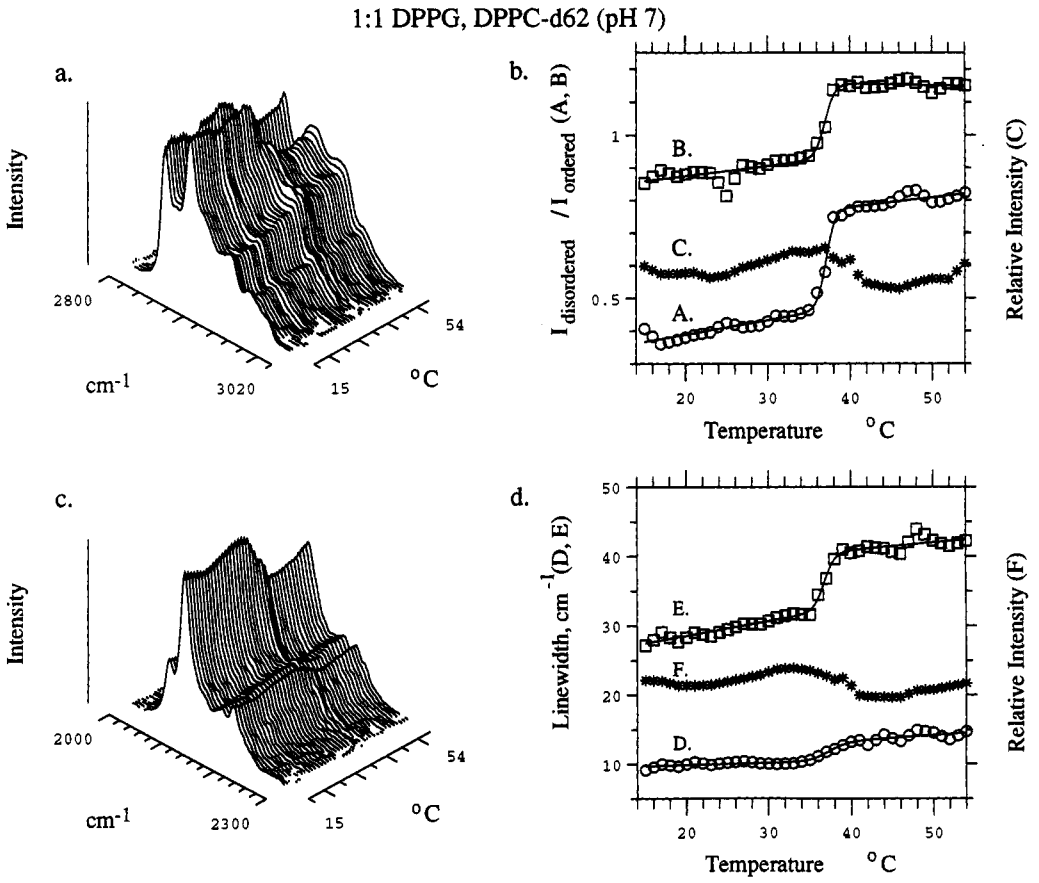

FIGURE 2: Raman spectra of DPPG in the C–H (2800–3000 cm^{-1}) and of DPPC-d_{62} in the C–D (2000–2300 cm^{-1}) stretching mode regions as a function of temperature. (a) Topological plot of the C–H stretching mode region for a phospholipid mixture (1:1) of DPPG and DPPC-d_{62} at pH 7.2 in isotonic saline solution. (b) Peak height intensity ratios: (A) I_{2935}/I_{2880}; (B) I_{2850}/I_{2880}. (C) Relative integrated intensity over the C–H stretching mode region. (c) Topological plot of the C–D stretching mode region for the 1:1 DPPG/DPPC-d_{62} lipid mixture at pH 7.2 in isotonic saline solution. (d) Line widths at $\Delta\nu_{1/2}$ (D) and $\Delta\nu_{7/8}$ (E) of the peak height of the 2103-cm^{-1} feature. Curve F displays the relative integrated intensity over the C–D stretching mode region. The lines were calculated using a two-state theory to fit the experimental points in A, B, D, and E.

essentially the same for both lipid component species in a comparison of the various spectral order/disorder parameters. This value lies between the T_M's of the individual pure multilamellar species. On the basis of T_M alone, homogeneous mixing with very little, if any, segregation of the lipids is implied. Because the T_M values derived for the lipid mixture are identical for the various spectral order/disorder indicators, a high correlation exists between the two inter- and intramolecular order/disorder parameters characterizing the phase transition; that is, during the phase transition the lattice expansion and acyl chain *trans/gauche* isomerization processes occur concurrently. The ΔT transition breadths are also nearly the same for the DPPG and DPPC-d_{62} species with the exception of the width of the lateral order/disorder parameter for the DPPC-d_{62} species which at 4.6 ± 1.1 °C is nearly twice the ΔT indicated by the other parameters. This decrease in the cooperativity of the DPPC-d_{62} lateral order/disorder parameter during the phase transition compared with that of DPPG implies neighboring inhomogeneities around the DPPC-d_{62} that could also indicate some lipid segregation or microdomain structures.

DPPG/DPPC-d_{62} Phospholipid Complexes with either KL_4 or DL_4. Figures 3 and 4 display as a function of temperature the Raman spectra and the specific peak height intensity ratio, line width, and integrated intensity parameters over the C–H and C–D stretching mode regions for the 1:1 mole ratio DPPG/DPPC-d_{62} phospholipid multilayers reconstituted separately with either the KL_4 or DL_4 polypeptides, respectively. The interactions of both peptides with the lipid mixture are sufficiently strong to broaden greatly the gel to liquid crystalline phase transitions. The transition temperatures T_M and the breadths of the transition ΔT can only be estimated as a range of temperatures and are listed in Table I. The integrated intensity curves of the DPPG C–H stretching mode region of the mixed lipid plus KL_4 system (Figure 3bC) first increase with temperature and, after reaching a maximum around 28 °C, then decrease, as expected, throughout the 30–50 °C temperature range with the exception of the 36–38 and 45–47 °C regions in which the intensity increases slightly. That is, the normal lateral bilayer expansion for the liquid-crystalline phase leads to a reduction in the band intensity for the C–H stretching region modes. The DPPG peak height intensity ratio I_{2935}/I_{2880} (Figure 3bA), corresponding to changes in both lateral chain–chain interactions and *gauche/trans* isomerizations begins to increase around 30 °C and generally continues until 48 °C. Some deviations occur around 39 and 42–45 °C which are also shared by the integrated intensity parameter and the pure interchain I_{2850}/I_{2880} order/disorder marker. The increase in the lateral order/disorder parameter (Figure 3bB) begins around 32 °C, approximately 4 °C above the I_{2935}/I_{2880} indicator. The phospholipid mixture (Figure 2) devoid of peptide shows deviations in intensity and the order parameters for both components in the 47–50 °C temperature range and suggests that this results in lipid matrix reorganizations that are not specific to the peptide interaction. These particular thermal events may be related to the large scattering intensity change observed in the pure DPPG multilayer system. The modifications in bilayer structure due

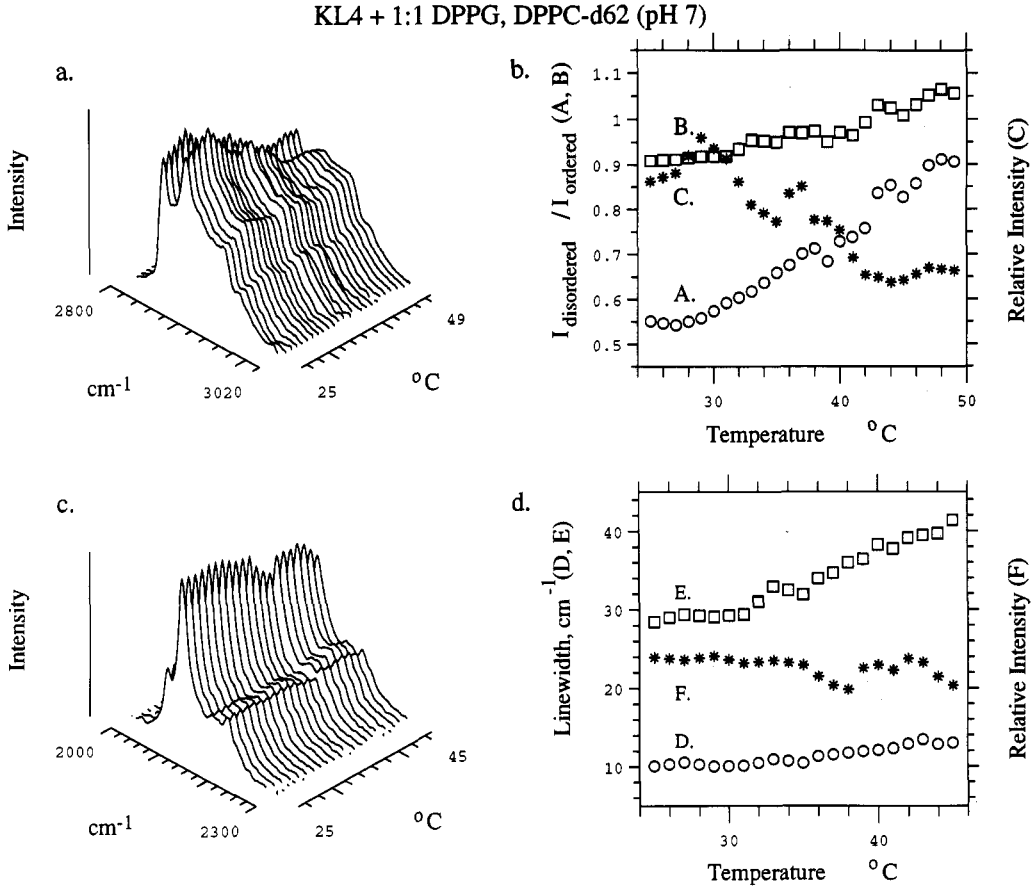

FIGURE 3: Raman spectra of DPPG in the C–H (2800–3000 cm^{-1}) and of DPPC-d_{62} in the C–D (2000–2300 cm^{-1}) stretching mode regions with KL_4 as a function of temperature. (a) Topological plot of the C–H stretching mode region for a phospholipid mixture (1:1) of DPPG and DPPC-d_{62} with 4.8 wt % KL_4 at pH 7.2 in isotonic saline solution. (b) Peak height intensity ratios: (A) I_{2935}/I_{2880}; (B) I_{2850}/I_{2880}. (C) Relative integrated intensity over the C–H stretching mode region. (c) Topological plot of the C–D stretching mode region for the 1:1 DPPG/DPPC-d_{62} lipid mixture with 4.8 wt % KL_4 at pH 7.2 in isotonic saline solution. (d) Line widths at $\Delta\nu_{1/2}$ (D) and $\Delta\nu_{7/8}$ (E) of the peak height of the 2103-cm^{-1} feature. Curve F displays the relative integrated intensity over the C–D stretching mode region.

to the peptide interaction are more evident in the breadth of the phase transition and the large value, 0.55, of the gel state ratio I_{2935}/I_{2880} compared with the value of 0.40 for the peptide-free system. From electrostatic considerations, the positively charged lysines of the KL_4 peptide are expected to interact predominantly with the negatively charged phosphate of the headgroup of the DPPG component of the lipid mixture. This general hypothesis is consistent with the behavior of the DPPC-d_{62} component. The corresponding C–D parameter, $\Delta\nu_{1/2}$ (Figure 3dE), for the introduction of *gauche/trans* conformers for the DPPC-d_{62} bilayer assembly begins to increase around 34 °C, close to the T_M for pure DPPC-d_{62} and 4–5 °C below that for the DPPG component. The lateral order parameter, $\Delta\nu_{7/8}$ (Figure 3dD), does not show a distinct phase transition but rather a line width fluctuation over the 35–45 °C temperature range. The primary effect of the KL_4 interaction with the DPPC-d_{62} component is to decrease greatly the cooperativity of the phase transition as measured by both disorder parameters. The line widths, and hence the intrinsic bilayer disorder of this species, are unchanged compared with the lipid mixture without peptide for both the gel and liquid-crystalline phases (see Table I). The more extensive modification by the KL_4 peptide of the multilamellar structural characteristics of the DPPG component compared to the DPPC-d_{62} species serves as a further indication of lipid segregation. In fact, the scatter in the temperature profiles of the peak height ratios of the DPPG component and the line widths of DPPC-d_{62} resemble poorly defined but authentic biphasic behavior. One transition occurs in the 32–36 °C region and the other from 40 to 42 °C, temperature ranges close to the T_M's of the pure lipid components. The extent of segregation may be not be sufficiently great to reflect distinct phase transitions for each component; however, each lipid component exhibits a distinctly different thermotropic behavior, suggesting segregated domains which are rich in one component or the other. The spectroscopic features indicating order/disorder are averaged in the Raman experiment over those molecules in a variety of environments. It is noteworthy to emphasize that the individual spectra are relatively noise-free and that the scatter in the peak height ratio and relative integrated intensity parameters as a function of temperature is due primarily to changes in the thermal and statistical molecular properties of the sample. That is, the scatter in the data is not indicative of spectral noise or instrumental fluctuations occurring during the acquisition of data.

Conventional electrostatic arguments also suggest that the negatively charged aspartic acid residues of the DL_4 peptide reconstituted in the liposomes at pH 7.2 would interact with the positively charged choline quaternary ammonium groups of the zwitterionic DPPC-d_{62} lipid to a greater extent than with the negatively charged DPPG species in the binary lipid mixture. The value, 0.60, of the I_{2935}/I_{2880} ratio for the lipid mixture + DL_4 (Figure 4bA) for the gel phase at 25 °C indicates considerable disorder and even a greater perturbation of the DPPG by DL_4 than the interaction of KL_4 with DPPG. This ratio increases until it reaches a value of 1.0 around 45 °C. Above this temperature, the ratio I_{2935}/I_{2880} is nearly the same as the I_{2850}/I_{2880} peak height intensity ratio indicating

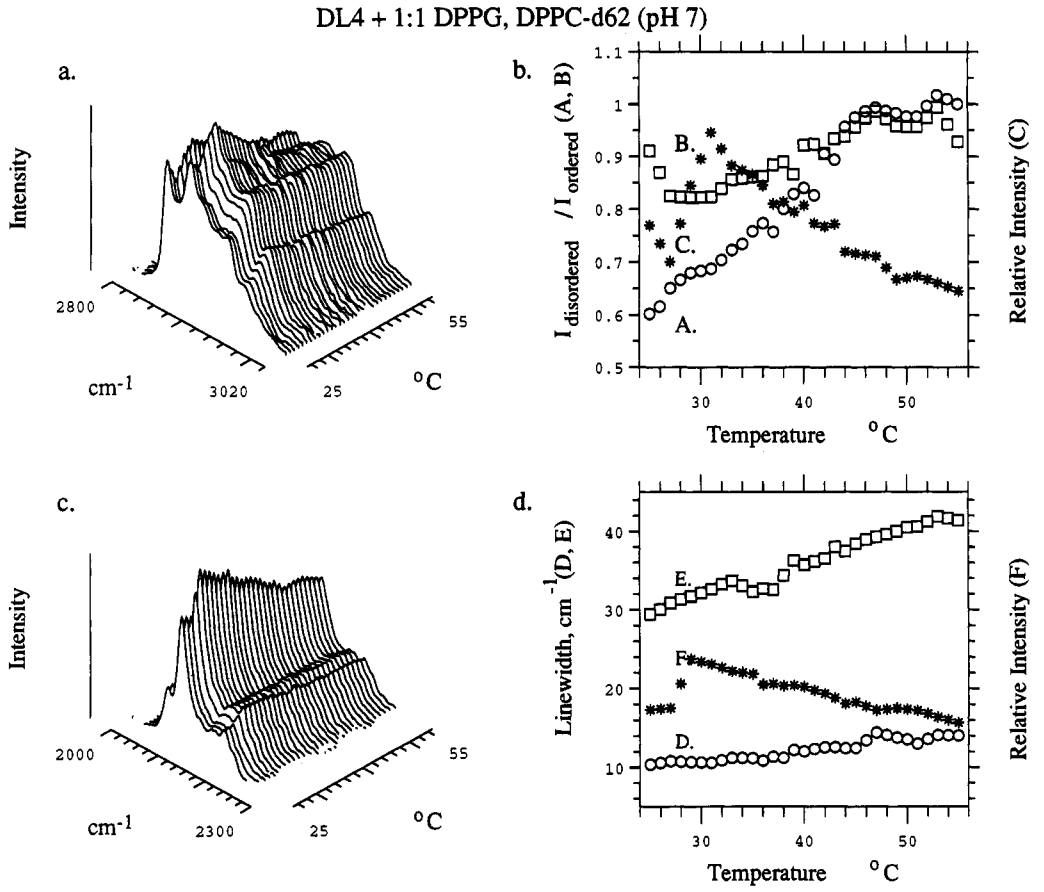

FIGURE 4: Raman spectra of DPPG in the C–H (2800–3000 cm^{-1}) and of DPPC-d_{62} in the C–D (2000–2300 cm^{-1}) stretching mode regions with DL_4 as a function of temperature. (a) Topological plot of the C–H stretching mode region for a phospholipid mixture (1:1) of DPPG and DPPC-d_{62} with 4.8 wt % DL_4 at pH 7.2 in isotonic saline solution. (b) Peak height intensity ratios: (A) I_{2935}/I_{2880}; (B) I_{2850}/I_{2880}. (C) Relative integrated intensity over the C–H stretching mode region. (c) Topological plot of the C–D stretching mode region for the 1:1 DPPG/DPPC-d_{62} lipid mixture with 4.8 wt % DL_4 at pH 7.2 in isotonic saline solution. (d) Line widths at $\Delta\nu_{1/2}$ (D) and $\Delta\nu_{7/8}$ (E) of the peak height of the 2103-cm^{-1} feature. Curve F displays the relative integrated intensity over the C–D stretching mode region.

considerable intramolecular disorder. A relatively intense 2935 cm^{-1} feature is observed when the terminal methyl group occupies an environment of increased polarity (Hill & Levin, 1979). The presence of water or DL_4 at the bilayer midplanes within the multilamellar assembly could increase the polarity of the region and thus increase the scattering of the 2935-cm^{-1} feature. This observation suggests an alteration in the structural integrity of the lipid bilayer. At pH 7, aspartic acid is negatively charged, and the interaction of the peptide with the bilayer yields an even more negatively charged bilayer surface than exists in the peptide-free system. The DPPG headgroups may separate slightly to relieve the electrostatic repulsion, which at higher temperatures would increase the individual bilayer disorder of the multilamellar dispersion and permit the incursion of water or DL_4 into the bilayer midplane. The relative integrated intensity curves (Figure 4, panels bC and dF) for both components of the lipid mixture increase fairly abruptly at temperatures below 30 °C and then decrease gradually with minor fluctuations from 35 to 48 °C. The DPPG/DL_4 lateral disorder parameter, I_{2850}/I_{2880}, also indicates a broad melting transition beginning around 32 °C and extending to about 44 °C, reflecting little phase change cooperativity and considerable lateral chain–chain disorder similar to that exhibited by pure DPPG, although not as great as indicated by the 1:1 DPPG/DPPC-d_{62} mixture. The lateral order/disorder parameter for the DPPC-d_{62} species (Figure 4dD) $\Delta\nu_{7/8}$ shows no distinct phase transition near the T_M for the individual components, but variations in this parameter occur around 47 and 52 °C, phenomena which are also observed in the peptide-free lipid mixture. The DPPC-d_{62} *gauche/trans* isomerization parameter $\Delta\nu_{1/2}$ also increases from its value of 30 cm^{-1} at 25 °C to 42 cm^{-1} at 53 °C with a dip in value around 35–40 °C, a temperature range encompassing the phase transition temperatures of both components. The line width measures of both order/disorder parameters for the deuterated acyl chains in the DPPC-d_{62} member of the DL_4 lipid mixture are similar in magnitude to those in the peptide-free lipid mixture for the liquid-crystalline and gel phases. No distinct phase transition is observed, but variations exist in the temperature profile which suggest that a small fraction of the DPPC-d_{62} portion may undergo a phase change, whereas the majority of the bulk DPPC-d_{62} lipid may exhibit a wide range of neighboring interactions manifest by the broad, noncooperative phase transition consistent with the disordered DPPG component. The spectral parameter indicative of both lateral and intramolecular order/disorder is increased greatly for the DPPG component due to the DL_4 interaction in the liquid-crystalline state compared to the peptide-free binary liposome and to the KL_4 reconstituted multilayers. Because the I_{2850}/I_{2880} spectral parameter for pure lateral order/disorder is not qualitatively dissimilar for the DL_4 and KL_4 reconstituted liposomes and the peptide-free binary mixture, the origin of the disorder for the DL_4 reconstituted multilayers indicated by the I_{2935}/I_{2880} parameter probably resides in an increase in the *gauche/trans* isomerization occurring during the phase transition.

DPPC-d_0 and DPPG-d_0 Multilayers Reconstituted with DL_4 and KL_4. In an attempt to determine the primary mode

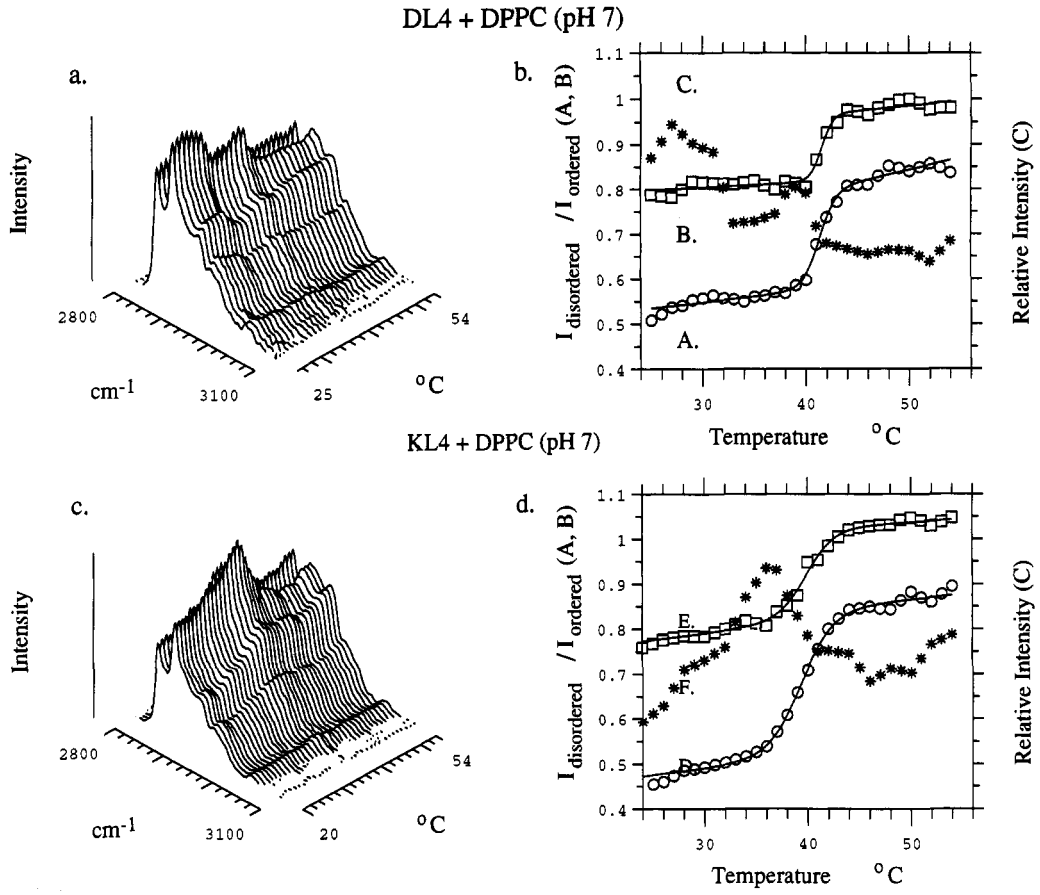

FIGURE 5: Raman spectra of DPPC-d_0 in the C–H (2800–3100 cm^{-1}) stretching mode region with DL_4 and KL_4, respectively, as a function of temperature. (a) Topological plot of the C–H stretching mode region for DPPC and a 9.5 wt % mixture of DL_4 in a pH 7.2 phosphate buffer and isotonic saline solution. (b) Peak height intensity ratios: (A) I_{2935}/I_{2880}; (B) I_{2850}/I_{2880}. (C) Relative integrated intensity over the C–H stretching mode region. (c) Topological plot of the stretching mode region for a mixture of DPPC and 9.5 wt % KL_4 in a pH 7.2 phosphate buffer and isotonic saline solution. (d) Peak height intensity ratios: (D) I_{2935}/I_{2880}; (E) I_{2850}/I_{2880}. Curve F displays the relative integrated intensity over the C–H stretching mode region.

of interaction of the peptides with the binary mixtures of DPPC and DPPG, both peptides were mixed separately with DPPC-d_0 and DPPG-d_0, and the thermotropic behavior of the C–H stretching mode region of the Raman scattering was explored. The topological plots and the peak height intensity ratios shown in the Figure 5 provide evidence that both peptides induce only minor perturbations to the DPPC multilayers. The similar data in Figure 6 for the peptides reconstituted with DPPG show a considerable increase in the perturbation of DL_4 to the DPPG structure but only a moderate perturbation to the thermotropic behavior due to the interaction of KL_4 with DPPG. A summary of the spectral properties for these four systems as well as the pure DPPC-d_0 is included in Table I. The main phase transition temperature T_M for DPPC is only suppressed by about 1.5 °C for the KL_4 peptide and by <1 °C for the DL_4 peptide in comparison with the peptide-free DPPC lipid. The increases in the widths of the phase transitions compared to the pure lipid indicate a decrease in the cooperativities of the gel to liquid crystalline phase changes. The spectral data resulting from the interaction of KL_4 with the DPPC matrix is that expected from an extrinsic peptide with positive groups electrostatically interacting with the phosphate portion of the DPPC zwitterion (Papahadjopoulos et al., 1975). Although T_M for the multilamellar vesicles changes very little and is accompanied by a decrease in the cooperativity, the peak height ratio difference from the gel to the liquid crystalline phase, an indicator of ΔS for the phase transition (Huang & Levin, 1983), is not greatly altered from that of the peptide-free lipid. In the DPPC+DL_4 reconstituted system, a large disorder of the bilayers is displayed in the gel phase I_{2935}/I_{2880} compared to either the pure lipid or the DPPC+KL_4 system. The gel state I_{2935}/I_{2880} disorder/order parameter for DPPC+DL_4 increases to 0.53 compared with 0.46 and 0.47 for the pure DPPC and DPPC+KL_4 multilamellar systems, respectively. Since the gel phase for this liposome is relatively disorderd, the phase transition for DPPC+DL_4 would manifest smaller entropy and enthalpy changes compared to the DPPC or DPPC+KL_4 multilayers. According to the relationships of Huang and Levin (1983) and Huang et al. (1982), the difference (ΔI_R) in the extrapolated I_{2935}/I_{2880} peak ratios at T_M between the gel and the liquid-crystalline phases is proportional to the entropy of the transition and inversely proportional to the effective acyl chain length. Using the plots from Huang et al. (1982), we ascertain that the effective acyl chain length of the DPPC+DL_4, based upon disorder/order spectral parameters, is slightly less than that of pure dimyristoylphosphatidylcholine (DMPC) multilayers, a shorter, symmetric 14-carbon chain lipid. It follows that the entropy change for the transition is correspondingly less, as well, because of the fewer *gauche/trans* isomerizations now involved in the phase transition. Above T_M the multilamellar disorder is nearly the same as the unperturbed system as determined by the I_{2935}/I_{2880} parameter. The lateral chain–chain order/disorder parameter I_{2850}/I_{2880} for the DPPC/peptide systems behaves in much the same fashion in both the gel and liquid-crystalline phases, as the pure lipid, indicating an essentially unperturbed lattice defined by interchain interactions.

The relatively small perturbation of both peptides on pure DPPC-d_0 multilayers indicates that the predominant pertur-

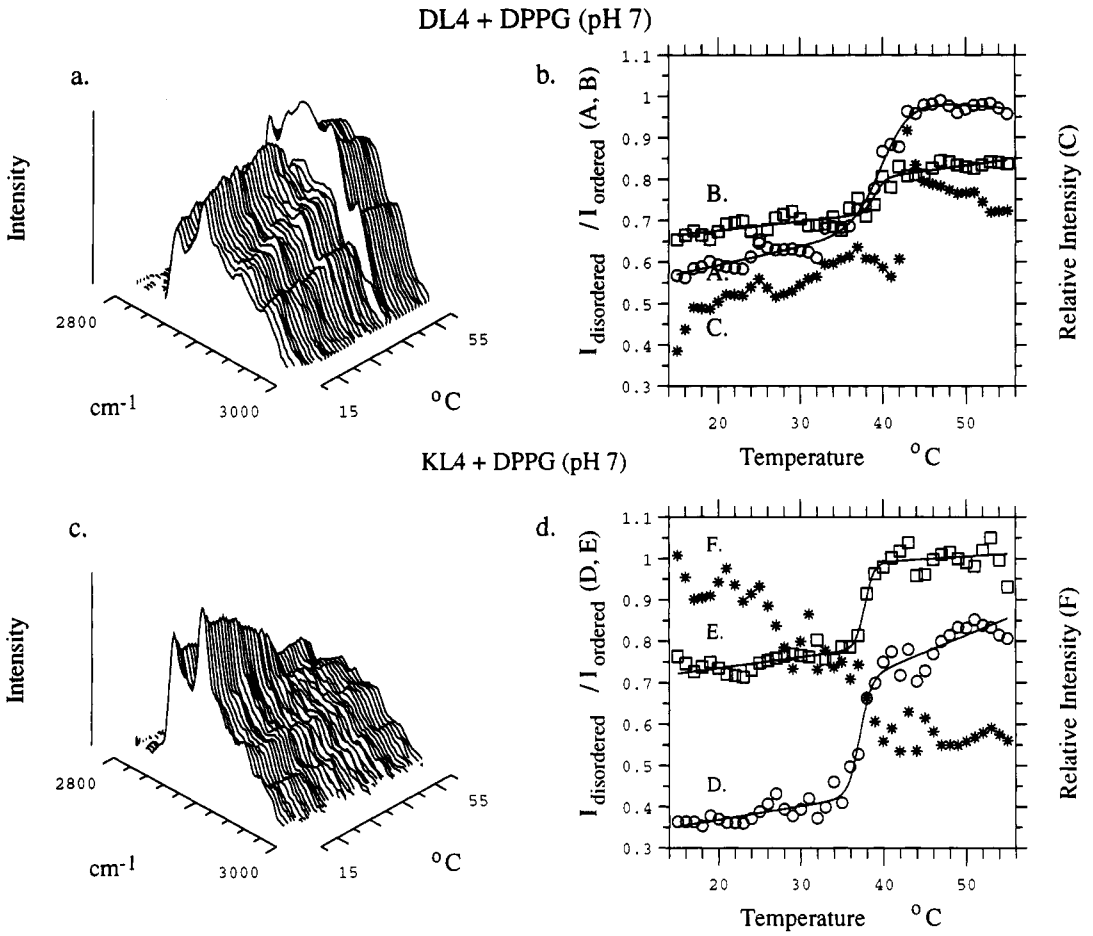

FIGURE 6: Raman spectra of DPPG-d_0 in the C–H (2800–3100 cm^{-1}) stretching mode region with DL_4 and KL_4, respectively, as a function of temperature. (a) Topological plot of the C–H stretching mode region for DPPG and a 9.5 wt % mixture of DL_4 in a pH 7.2 phosphate buffer and isotonic saline solution. (b) Peak height intensity ratios: (A) I_{2935}/I_{2880}; (B) I_{2850}/I_{2880}. (C) Relative integrated intensity over the C–H stretching mode region. (c) Topological plot of the stretching mode region for a mixture of DPPG and 9.5 wt % KL_4 in a pH 7.2 phosphate buffer and isotonic saline solution. (d) Peak height intensity ratios: (D) I_{2935}/I_{2880}; (E) I_{2850}/I_{2880}. Curve F displays the relative integrated intensity over the C–H stretching mode region.

bation of both peptides with the DPPG/DPPC-d_{62} multilayer arises from the specific interaction of the individual peptides with the DPPG bilayer headgroup. This conjecture is confirmed by the results shown in Figure 6 illustrating the spectral curves and peak height ratios for the peptides, DL_4 and KL_4, mixed with DPPG. The I_{2935}/I_{2880} spectral parameters for DPPG+DL_4 multilayers are similar to the gel and liquid-crystalline phase disorder/order values for the binary lipid mixture with DL_4. The DPPG+DL_4 system, by contrast, has a distinct phase transition at 40.1 ± 0.4 °C, nearly the same as the phase transition of pure DPPG. The large peak height ratio for the liquid-crystalline phase indicates an acyl chain environment with a high polarity (Hill & Levin, 1979), a condition which would result if either water or DL_4 were to migrate to the acyl chain region. The low value, 0.68, for the pure lateral order parameter, I_{2850}/I_{2880}, suggests that the acyl chains are highly ordered and interdigitated in the gel phase (O'Leary & Levin, 1984). The interaction of the negatively charged peptide with the negative surface charge of the lipid spreads the headgroups permitting partial interpenetration of the acyl chains. The integrated intensity of the DPPG+DL_4 Raman CH stretching mode spectral region also increases at a temperature close to the high end of the phase transition. The different behavior of the order/disorder parameters due to the interaction of either KL_4 or DL_4 with the DPPG species, in comparison to the effects on the DPPC-d_{62} component of the lipid mixture, again suggests lipid segregation.

Previous Raman spectroscopic work of multilamellar assemblies suggested a model for the peptide–phospholipid complex in which the hydrophilic peptides interact with the charged phosphatidylglycerol headgroup components of the bilayer, forming a more constrained lipid matrix than that of the peptide-free system (Vincent et al., 1991). The peptide–headgroup associations inhibited lipid lateral diffusion inducing the formation of small, laterally segregated domains with increased PG concentrations. These same considerations apply with modification to the systems in which KL_4 and DL_4 interact with the mixed DPPC-d_{62}/DPPG multilamellar lipid system, leading to small, laterally segregated domains. These segregated units continually change in time, providing a dynamic interpretation of neighboring interactions in terms of the number and type of molecules at the domain boundaries. Since the number of identical units required to define a cooperative event is small, the observed broad, poorly defined phase transitions result. For reconstituted mixed multilayers with DL_4 and KL_4, the predominant peptide interaction is with the DPPG component of the mixture, leading, in the case of DL_4, to individual bilayer disruption through an increase in the negative surface charge. Cochrane and Revak (1991) noted that DL_4 was a far less effective surfactant than KL_4, as determined by the bubble surfactometer, although addition of DL_4 slightly reduced the surface tension of the system in comparison to the properties of the pure lipid. The reason for this activity was presumed to be due to the weak interaction of DL_4 with the quaternary ammonium choline groups of

DPPC. However, in view of the enhanced 2935-cm^{-1} Raman spectral region, it appears that DL_4 disrupts the bilayers in the liquid-crystalline phase, leading perhaps to its failure as an effective surfactant. KL_4, however, was found to be nearly as effective a surfactant additive as SP-B residues in increasing the compliance in fetal rabbits (Cochrane & Revak, 1991). The results of the bubble surfactometer, surface tension balance, and increase in fetal rabbit lung compliance suggested in the earlier work (Vincent et al., 1991; Cochrane & Revak, 1991) represent physiological measures which were thought to correlate work the spectroscopic data in terms of the ability of the surfactant peptides to enhance lipid bilayer chain order in multilamellar assemblies. The results presented here imply that lipid domain structures are probably present in effective surfactants and that the dynamic bilayer microheterogeneity induced by the surfactant peptide or protein may be essential for physiological activity. Peptide perturbations which broaden the phase transitions in these model surfactant systems apparently are not sufficient to destroy their physiological efficacy. However, perturbations strong enough to disrupt the liquid-crystalline bilayer structure may produce noncompliant surfactants.

The fluorescence anisotropy measurements of Baatz et al. (1990, 1991) also indicated that SP-B and SP-B 53-78 interact specifically with the phosphatidylglycerol component of the lipid mixture and increase the order of the headgroup portion of the lipid. Carrier and Pézolet (1984) showed that, in multilamellar complexes of DPPG and poly(L-lysine) (150 000 MW), evidence exists for lipid segregation when the mole fraction of the lysine residue/DPPG is less than 1. In addition, the poly(L-lysine) (PLL) complex with DPPG (lysine residue/DPPG mole ratio equal to 1) has a slightly higher T_M and a more ordered gel state, indicating that the PLL interaction with the DPPG holds the headgroups together to stabilize the lipid bilayer. Broad noncooperative phase transitions in pure lipid systems have also been observed. For pure phospholipid systems in which the *sn*-1 chain is saturated and the *sn*-2 chain contains four or six double bonds, Litman et al. (1991) attribute the broad gel to liquid crystalline phase transitions to the decreased cooperativity induced by the microclusters of lipids.

SUMMARY

The thermotropic behavior of the reconstituted multilamellar lipid dispersions of a 1:1 phospholipid mixture of dipalmitoylphosphatidylcholine-d_{62} and dipalmitoylphosphatidylglycerol with the pulmonary surfactant related peptides KL_4 and DL_4 show profound effects on the lipid bilayer gel and liquid-crystalline phase order/disorder characteristics and the phase transition cooperativity properties originating from the lipid/peptide interactions. Associations of the 21 amino acid residue KL_4 and DL_4 peptides to the liposomal surfaces increases bilayer disorder in both the gel and liquid-crystalline phases of the multilayers and decreases the cooperativity of the gel to liquid crystalline transitions to the extent that the transitions extend over a span of nearly 20 °C. This is particularly evident for the DPPG component of the lipid mixture in which the parameter monitoring simultaneously both inter- and intrachain interactions (I_{2935}/I_{2880}) and the parameter sensing pure chain–chain interactions (I_{2850}/I_{2880}) exhibit a decrease in the cooperativity of the bilayer melting process. The KL_4 peptide interacts more strongly with the DPPG component than with the DPPC-d_{62} component of the binary lipid mixture as would be expected from purely electrostatic considerations. Since within the multilayers the positively charged amine of the lysine interacts with the negatively charged phosphate moiety of the DPPG headgroup to reduce the surface charge, the bilayer stabilizes to a greater extent than the bilayer interaction with the corresponding DL_4 peptide. Interestingly, the DL_4 peptide–lipid complex also interacts strongly with the DPPG component and shows a great decrease in phase transition cooperativity in terms of the DPPG I_{2935}/I_{2880} index, which emphasizes the *gauche*/*trans* isomerization process during the phase transition. Furthermore, the disorder of liquid-crystalline state in terms of the I_{2935}/I_{2880} parameter is much greater than that of the KL_4 lipid complex. The addition of the negatively charged DL_4 aspartate groups to the lipid headgroup region of the bilayer would lead to an overall increase in the negative surface charge, thus increasing the repulsion between lipid headgroups and destabilizing the individual bilayer. The disruption in the multilamellar dispersions of the lipid bilayer by DL_4, which would permit water or DL_4 to penetrate into the bilayer midplane, could prevent the uniform coating of a surface by surfactant, which, in turn, would provide little or no resistance to the surface tension of water and lead to an ineffective surfactant. Additional interactions other than the simple electrostatic interactions of the positive quaternary ammonium and amine groups with the negative phosphate and carboxyl groups may be involved; clearly, considerations such as hydrogen bonding, the size of the amino acid side group, compensating counterions, and waters of hydration must be taken into account in order to fully describe the spectroscopic properties of these multilayer systems.

ACKNOWLEDGMENT

J.S.V. and I.W.L. acknowledge valuable discussions with Drs. Ralph Adams and Neil Lewis regarding various aspects of this work. Mr. John Powell of DCRT, NIH was responsible for developing the graphical presentation programming module used in this study.

REFERENCES

Baatz, J. E., Elledge, B., & Whitsett, J. A. (1990) *Biochemistry 29*, 6714–6720.

Baatz, J. E., Sarin, V., Absolom, D. R., Baxter, C., & Whitsett, J. A. (1991) *Chem. Phys. Lipids 60*, 163–178.

Boggs, J. M. (1980) *Can. J. Biochem. 58*, 755–770.

Boggs, J. M. (1987) *Biochim. Biophys. Acta 906*, 353–404.

Bryant, G. F., Lavialle, F., & Levin, I. W. (1982) *J. Raman Spectrosc. 12*, 118–121.

Carrier, D., & Pézolet, M. (1984) *Biophys. J. 46*, 497–506.

Cevc, G., Watts, A., & Marsh, D. (1980) *FEBS Lett. 120*, 267–270.

Clements, J. A. (1977) *Am. Rev. Respir. Dis. 115*, 67–71.

Cochrane, C. G., & Revak, S. D. (1991) *Science 254*, 566–568.

Devlin, M. T., & Levin, I. W. (1990) *J. Raman Spectrosc. 21*, 441–452.

Eibl, H., & Wooley, P. (1979) *Biophys. Chem. 10*, 261–271.

Findlay, E. J., & Barton, P. G. (1978) *Biochemistry 17*, 2400–2405.

Harwood, J. L., & Richards, R. J. (1985) *Mol. Aspects Med. 8*, 423–514.

Hill, I. R., & Levin, I. W. (1979) *J. Chem. Phys. 70*, 842–851.

Huang, C., & Levin, I. W. (1983) *J. Phys. Chem. 87*, 1509–1513.

Huang, C., Lapides, J. R., & Levin, I. W. (1982) *J. Am. Chem. Soc. 104*, 5926–5930.

Jacobson, K., & Paphadjopoulos, D. (1975) *Biochemistry 14*, 152–161.

Kirchhoff, W. H., & Levin, I. W. (1987) *J. Res. Natl. Bur. Stand. (U.S.) 92*, 113–128.
Levin, I. W. (1984) *Adv. Raman Spectrosc. 11*, 1–49.
Levin, I. W. (1985) *Chemical, Biological and Industrial Applications of Infrared Spectroscopy* (Durig, J. R., Ed.) pp 173–197, John Wiley and Sons, New York.
Litman, B. J., Lewis, E. N., & Levin, I. W. (1991) *Biochemistry 30*, 313–319.
Mendelsohn, R., & Maisano, J. (1978) *Biochim. Biophys. Acta 506*, 192–201.
Mendelsohn, R., & Taraschi, T. (1978) *Biochemistry 17*, 3944–3949.
Mendelsohn, R., & Koch, C. C. (1980) *Biochim. Biophys. Acta 598*, 260–271.
Merrifield, R. B. (1963) *J. Am. Chem. Soc. 85*, 2149–2154.
O'Leary, T. J., & Levin, I. W. (1984) *Biochim. Biophys. Acta 776*, 185–189.
Papahadjopoulos, D., Moscarello, M., Eylar, E. H., & Isac, T. (1975) *Biochim. Biophys. Acta 401*, 317–335.
Pascher, I., & Sundell, S. (1986) *Biochim. Biophys. Acta 855*, 68–78.
Pascher, I., Sundell, S., Harlos, K., & Eibl, H. (1987) *Biochim. Biophys. Acta 896*, 77–88.
Persson, A., Chang, D., & Crouch, E. (1990) *J. Biol. Chem. 265*, 5755–5760.
Revak, S. D., Merritt, T. A., Hallman, M., & Cochrane, C. G. (1986) *Am. Rev. Respir. Dis. 134*, 1258–1265.
Revak, S. D., Merritt, T. A., Degryse, E., Stefani, L., Courtney, M., Hallman, M., & Cochrane, C. G. (1988) *J. Clin. Invest. 81*, 826–833.
Revak, S. D., Merritt, T. A., Hallman, M., Heldt, G., La Polla, R. J., Hoey, K., Houghten, R. A., & Cochrane, C. G. (1991) *Pediatr. Res. 29*, 460–465.
Scarpelli, E. M. (1988) *Surfactants and the Lining of the Lung*, Johns Hopkins Press, Baltimore, MD.
Van Dijck, P. W. M. (1979) *Biochim. Biophys. Acta 555*, 89–101.
Van Dijck, P. W. M., de Kruijff, B., Verkleij, A. J., van Deenen, L. L. M., & de Gier, J. (1978) *Biochim. Biophys. Acta 512*, 84–96.
Vincent, J. S., & Levin, I. W. (1991) *Biophys. J. 59*, 1007–1021.
Vincent, J. S., Revak, S. D., Cochrane, C. G., & Levin, I. W. (1991) *Biochemistry 30*, 8395–8401.
Watts, A., Harlos, K., Maschke, W., & Marsh, D. (1978) *Biochim. Biophys. Acta 510*, 63–74.